AUGER ELECTRON SPECTROSCOPY OF ALLOY SURFACES

S. H. Overbury and G. A. Somorjai

Inorganic Materials Research Division, Lawrence Berkeley Laboratory
and Department of Chemistry; University of California
Berkeley, California

ABSTRACT

Regular solution models predict surface segregation of the constituent of lowest surface free energy in homogeneous multicomponent systems. Analysis of the Auger electron emission intensities from alloys yield the surface composition and the depth distribution of the composition near the surface. Auger Electron Spectroscopy (AES) studies of the surface composition of the Ag-Au and Pb-In systems have been carried out as a function of bulk composition and temperature. Although these alloys have very different regular solution parameters their surface compositions are predictable by the regular solution models.

NOTICE
This report was prepared as an account of work sponsored by the United States Government. Neither the United States nor the United States Energy Research and Development Administration, nor any of their employees, nor any of their contractors, subcontractors, or their employees, makes any warranty, express or implied, or assumes any legal liability or responsibility for the accuracy, completeness or usefulness of any information, apparatus, product or process disclosed, or represents that its use would not infringe privately owned rights.

MASTER

1) INTRODUCTION

The composition of multicomponent systems at the topmost surface layer determines to a large extent their resistance to external chemical attack and their catalytic activity in surface reactions. Simple thermodynamic arguments[1] indicate that the surface composition of alloys should be different from their composition in the bulk. In order to minimize the positive total surface free energy of the multicomponent system, the constituent of lowest surface free energy will accumulate in the topmost surface layer.[2]

It has been possible only recently with the advent of Auger electron spectroscopy (AES)[3,4] and other surface sensitive techniques (ESCA, ISS, etc.) to analyze the composition of the surface layer of alloys. Thus, we can now verify, by experiment, the thermodynamic relationships that govern the surface composition of these systems. If we can employ a thermodynamic model, such as the regular solution model for example, to compute the composition of an alloy surface, we may use this model with confidence to predict the surface composition of at least one class of alloys for a wide range of bulk compositions and temperature.

This paper reports on AES experiments aimed at determining the surface composition of homogeneous binary alloys as a function of bulk composition and temperature. It appears that the experimental data for the Pb-In and Ag-Au systems are in good agreement with the surface compositions predicted by a regular solution model. Thus, for this class of systems, i.e., homogeneous binary alloys, the surface composition may be calculated with some degree of confidence.

2) THERMODYNAMIC MODELS TO PREDICT THE SURFACE COMPOSITION OF HOMOGENEOUS BINARY SOLUTIONS

The ideal solution theory assumes that the heat of mixing, ΔH_m of component A with component B is zero while the entropy of mixing is calculated assuming that the constituents are distributed randomly throughout the solution.[5] The surface is assumed to be composed of the topmost layer only (monolayer) although in some cases this approximation is relaxed.[6] Using this ideal solution monolayer model, the surface composition of the binary mixture can be expressed as

$$\frac{X_s^A}{X_s^B} = \frac{X_b^A}{X_b^B} \exp\left(\frac{(\sigma^B - \sigma^A)a}{RT}\right) \qquad (2.1)$$

where X_s^A and X_s^B are the atom fractions of the two components at the surface; X_b^A and X_b^B are the atom fractions of the two components in the bulk (below the topmost layer); σ^A and σ^B are the surface free energies (surface tensions) of the pure components A and B; and $\underline{a}$ is the average molar surface area. T is the absolute temperature and R is the gas constant. This model predicts that the constituent with the lower surface free energy accumulates on the surface, and that the surface composition of the mixture depends exponentially on the surface tension difference. In addition, this model predicts also that unlike the bulk composition, the surface composition is strongly dependent on temperature. The surface composition approaches the bulk composition exponentially with increasing temperature. The regular solution model takes into account the finite value of the heat of mixing, ΔH_m, that is given by

$$\Delta H_m = \Omega X \ (1-X) = Nz \left[E_{AB} - \frac{E_{AA} + E_{BB}}{2}\right] X_b \ (1-X_b) \qquad (2.2)$$

where Ω is the regular solution parameter which can be expressed in terms of the bond energies E_{ij}, Avogadro's number N and the bulk coordination number z. For example, both Pb-In and Ag-Au systems are fairly regular, their heat of mixing is expressed as[7]

$$\Delta H_m \approx 3850\ X^{Pb}(1-X^{Pb})\ \text{joules/mole} \qquad (2.3)$$

$$\Delta H_m = -(20{,}300-3350\ X^{Au})\ X^{Au}(1-X^{Au})\ \text{joules/mole} \qquad (2.4)$$

For the Pb-In system ΔH_m and, thus, Ω are positive and relatively small while for the Ag-Au system ΔH_m is exothermic (Ω is negative) and fairly large. The surface composition in the regular solution monolayer approximation is given by[8]

$$\frac{X_s^A}{X_s^B} = \frac{X_b^A}{X_b^B}\ \exp\left[\frac{(\sigma^B - \sigma^A)a}{RT}\right]\ \exp\left\{\frac{\Omega(\ell+m)}{RT}\left[(X_b^B)^2-(X_b^A)^2\right] + \frac{\Omega\ell}{RT}\left[(X_s^A)^2-(X_s^B)\right]\right\} \qquad (2.5)$$

The packing parameter $\underline{\ell}$ gives the fraction of nearest neighbors in the same plane while $\underline{m}$ is the fraction of nearest neighbors that are in an adjacent plane. For a face centered cubic lattice, a bulk atom has 12 nearest neighbors. Thus, for an atom in the (111) crystal face, there are 6 neighbors in the surface plane ($\ell = 6/12$) and three nearest neighbors in the plane below the surface, ($m = 3/12$). In this approximation, the surface composition becomes a fairly strong function of the heat of mixing, its sign, and magnitude in addition to the exponential dependence on the surface tension difference and temperature.

Williams[6] has extended the monolayer regular solution model by allowing the first four layers from the surface layer inward to have variable concentrations, but all layers deeper than the fourth are constrained to have the bulk composition. Assuming again that the solution is regular allows him to derive four coupled equations involving the atom fractions at each layer and the bulk atom fractions. The equations are

$$(\sigma^A-\sigma^B)a + RT\,\ell n\left[\frac{X_1(1-X_b)}{X_b(1-X_1)}\right] + 2\Omega\,(X_b-\ell X_1-\tfrac{1}{2}m-mX_2) = 0 \qquad (2.6a)$$

$$RT\,\ell n\left[\frac{X_2(1-X_b)}{X_b(1-X_2)}\right] + 2\Omega\,(X_b-\ell X_2-mX_1-mX_3) = 0 \qquad (2.6b)$$

$$RT\,\ell n\left[\frac{X_3(1-X_b)}{X_b(1-X_3)}\right] + 2\Omega\,(X_b-\ell X_3-mX_2-mX_4) = 0 \qquad (2.6c)$$

$$RT\,\ell n\left[\frac{X_4(1-X_b)}{X_b(1-X_4)}\right] + 2\Omega\,(X_b-\ell X_4-mX_3-mX_b) = 0 \qquad (2.6d)$$

here X_1 refers to the atom fraction of component A in the first layer, X_2 is the atom fraction of the same component in the second layer, etc. All other symbols are defined earlier.

It should be noted that equation 2.6a becomes the same as equation 2.5 when the second, third, and fourth layer compositions are set equal to X_b, that is, these equations reduce to the monolayer model as they should. This process is completely general and in fact similar expressions can be derived involving any number of layers of variable composition obtaining one equation for each layer. Solving equation 2.6 gives the atom fractions of both components in each atomic layer of the solid. This way, we can determine the depths profile or as we will refer to it, the equilibrium depth distribution (of composition). These calculations have been performed for a (111) face using the surface free energy values given in the literature for Pb, In, Ag and Au[8,10] and the results of these are plotted in Figures 1, 2, and 3.

Due to the lower surface free energy of Pb, the monolayer model and the multilayer model sensibly predict a considerable enrichment of Pb in the top layer. For Pb-In the regular solution parameter is positive which means that Pb-Pb and In-In bonds are stronger than Pb-In bonds. This results in "clustering" of Pb near the surface. Thus the multilayer model predicts also an enrichment in Pb in the 2nd, 3rd, and 4th layers, the magnitude of the enrichment decreasing rapidly toward the bulk.

The calculations give somewhat different results for the Ag-Au system. In this case both models predict an enrichment in Ag in the top layer as before. However, since for Ag-Au the regular solution parameter is negative (Ag-Ag and Au-Au bonds are not as strong as Ag-Au bonds), layering is obtained from the 4-layer model. The first layer is enriched in Ag at the expense of the second layer which is enriched in Au. The third layer then is enriched in Ag. The magnitude of this enrichment and depletion decreases rapidly toward the bulk. Thus, these calculations indicate that due to the large attractive interaction between Au and Ag, the regular solution model may not apply accurately and the Ag enrichment at the surface might well be accompanied by Au enrichment in the second layer. It should be noted that the surface composition is also strongly temperature dependent. With increasing temperature, the surface excess concentration diminishes rapidly.

3) ANALYSIS OF THE AUGER PEAK INTENSITIES TO OBTAIN SURFACE COMPOSITION AND DEPTH DISTRIBUTION

AES is one of the surface sensitive techniques that can be applied to monitor the surface composition of multicomponent systems.[3] The depth below the surface that is probed by low energy electrons (50-600 electron volts), that is, the useful energy range of Auger electrons, is of the same order of magnitude as the expected depth of surface enrichment. Therefore, the intensities of the Auger spectral peaks should contain information on the depth distribution. Careful measurements of intensity ratios, i.e., ratios of the intensities of an Auger peak at one energy divided by the intensity of the Auger peak at another energy, should yield this information. It should be pointed out that the data collected in this manner requires little in the way of absolute calibration and some effects due to the depth distribution can be observed with no calibration necessary whatsoever.

To predict the intensity ratio, the assumption will be made that Auger transitions are excited uniformly with depth. For pure solids this should be a good approximation since the much higher energy incident electron beam is considered to have a much larger attenuation depth than the observed Auger electron. This approximation is also aided by the fact that the average electron energy loss in a solid per collision is small, about 15 electron volts, so that the incident electron of 2000 eV energy may undergo several collisions but still excite Auger transitions with considerable efficiency. Therefore if P_1 and P_2 are the probabilities of seeing an atom at depth d_1 and d_2 respectively, then

$$\frac{P_1}{P_2} = \frac{\exp\left(-d_1/\lambda_E\right)}{\exp\left(-d_2/\lambda_E\right)} \qquad (3.1)$$

where λ_E is the attenuation depth of the observed electrons of energy E defined in terms of a Beer's Law type attenuation. Consequently, for a pure solid the Auger peak intensity I_E at energy E can be written as

$$I_E = \int_0^\infty \kappa(E,\ldots) \exp \ (-z/\lambda_E) \ dz \tag{3.2}$$

Where $\kappa(E,\ldots)$ is a complicated function involving properties of the solid, the electron scattering within it, and all experimental parameters. This expression serves to break the Auger intensity into contributions from various depths z and to sum them. For a pure solid, using the assumption given above, integration of equation 3.2 yields

$$I_E = \kappa(E,\ldots) \ \lambda_E \tag{3.3}$$

In order to measure Auger peak intensities as a function of depth for an alloy, two further assumptions will be made. The first is that the presence of neighboring atoms does not effect the Auger yields. That is, there are no matrix effects. Therefore, the Auger intensity arising from a particular depth will depend only on the number of emitters.

The second assumption is that the escape depths of an electron does not depend upon the medium, but only upon the energy. This was shown experimentally to be approximately correct and many "universal" curves of escape depth versus energy have been published.[9] These assumptions lead to the equation

$$I_E = \kappa(E,\ldots) \int_0^\infty X(z) \exp \ (-z/\lambda_E) \ dz \tag{3.4}$$

that X(z) is the atom fraction of the emitting species at the depth z (the depth distribution).

For a pure solid exhibiting two Auger peaks at energies E and E' the ratio $R^0_{E,E'}$ becomes

$$R^0_{E,E'} \equiv \frac{I^0_E}{I^0_{E'}} = \frac{\kappa(E,\ldots)\lambda_E}{\kappa(E',\ldots)\lambda_{E'}} \tag{3.5}$$

and this ratio is easily measured. The superscript zero is used to denote intensities and ratios from pure metals. For an alloy the corresponding ratios are

$$R_{E,E'} = \frac{I_E}{I^0_{E'}} = \frac{\kappa(E,\ldots)}{\kappa(E',\ldots)} \frac{\int_0^\infty X(z)\,\exp\,(-z/\lambda_E)\,dz}{\int_0^\infty X(z)\,\exp\,(-z/\lambda_E)\,dz} \tag{3.6}$$

can also be easily measured. Therefore,

$$\frac{R_{E,E'}}{R^0_{E,E'}} = \frac{\lambda_{E'}}{\lambda_E} \frac{\int_0^\infty X(z)\,\exp\,(-z/\lambda_E)\,dz}{\int_0^\infty X(z)\,\exp\,(-z/\lambda_{E'})\,dz} \tag{3.7}$$

depends only upon the depth distribution and escape depths which in many cases are known or may be estimated. The right-hand side of 3.7 can therefore be calculated for various theoretical depth distributions. It should be noted that if there is no depth distribution, then $X(z) = X_b$ and it follows from equation 3.7 that $R_{E,E'} = R^0_{E,E'}$. Therefore, a change in the ratios of two Auger peaks arising from the same component in an alloy would be indicative of surface segregation of some sort. This same procedure can also be used for comparing Auger peak intensities of the two alloy components such as the ratio of intensity of an Au Auger peak with that of an Ag Auger peak.

In order to reveal surface segregation, if present, or compare the experimentally detected intensity ratios with those predicted by the various models, the Auger peak intensity data that is obtained for the different alloy compositions can be plotted various ways.

a) One may plot the intensity ratios of two Auger peaks, one for each component of the alloy, $R_{E,E'}(= I_A(E)_{alloy}/ I_B(E')_{alloy})$ divided by the intensity ratios of the same two Auger peaks of the pure metals, $R^o_{E,E'}(= I_A(E)_{pure}/ I_B(E')_{pure})$, that is $R_{E,E'}/ R^o_{E,E'}$ as a function of the bulk atom fraction ratio X^A_b/ X^B_b. Plotting the data in this way, values for an alloy having no surface segregation would fall on a line with slope equal to one. If one component is accumulated at the surface and there is a depth distribution of composition near the surface that is different from the bulk composition, the experimental data will lie above or below this "bulk ratio" line.

b) Another way of displaying the experimental Auger peak intensity data to reveal surface segregation is by plotting the ratio of intensities of two Auger peaks of the same component in the same alloy, (I_A (E) alloy/ I_B (E') alloy) as a function of the bulk atom fraction. If the surface composition changes the same way as the bulk composition does, this ratio would be constant. Surface segregation would be indicated by the systematic variation of this intensity ratio with alloy composition in a nonlinear manner.

c) A third method to identify surface segregation is by the summation of the intensity ratios

$$\frac{I_A(E)\text{ alloy}}{I_A(E)\text{ pure}} + \frac{I_B(E')\text{ alloy}}{I_B(E')\text{ pure}}$$

Since the two Auger peaks are at different electron energies E and E', they sample the composition over different depths in the alloy. Thus if the sample is homogeneous, in the absence of surface segregation, these intensity ratios will reflect precisely the bulk composition and their sums should be unity. However, if there is surface segregation then the intensity ratios will not reflect the bulk ratios and their sum may be greater or less than unity.

In addition to these types of data analysis the presence of temperature dependence of the Auger intensity ratios is an indication of changes in the surface composition.

4) RESULTS AND DISCUSSION

We have studied the Pb-In and Ag-Au systems by AES in some detail. The Pb-In system was studied in the liquid state to assure equilibration of the bulk and the surface phases. The Ag-Au alloy samples had to be heated to 300°C for over 30 minutes or to above this temperature for shorter times, after suitable cleaning of the surface of impurities (carbon, sulfur and chlorine) by ion sputtering, before equilibration of the surface phase and the bulk phase was achieved. The details of the AES experiments for both of these systems are described elsewhere.[10,11] In Figure 4 the Pb-In Auger peak intensity ratios are plotted as a function of the bulk atom fraction ratio on a log-log graph according to the first method of data analysis that was described above. All of the experimental points fall below the bulk ratio line indicating surface segregation of Pb as predicted by the regular solution models. In addition, the surface segregation decreases with increasing temperature as shown by the data points in Figure 4, as predicted by the regular solution models for this system.

The same plot of normalized Au-Ag Auger peak intensity ratios as a function of their atom fraction ratios are shown in Figures 5 and 6 for two different Auger peaks of gold. The solid lines indicate the trend as predicted for the various thermodynamic models. The 4-layer and the monolayer regular solution models give very similar predicted values and the experimental data appears to fit closely to the regular solution model. Unfortunately, the temperature required for achieving surface-bulk equlibration was too high (300°C) to allow a reliable study of the temperature dependence of the surface composition as was carried out for the Pb-In system.

To demonstrate our second method of analysis, i.e. plotting the ratio of two Auger peak intensities of the same component in the same alloy versus bulk composition, the values predicted by regular solution theory for such a ratio are given in Figure 7. Thus the presence of surface segregation in a binary alloy should show up as a deviation in ratios of this type. The third method of analysis listed above is demonstrated in Figure 8. This figure illustrates that the sum of normalized intensities from both components would not sum to unity for a system obeying the regular solution model. By normalized intensity is meant the intensity obtained from an alloy divided by the intensity from a pure reference.

Detailed studies of the Ni-Au[12] and Cu-Al[13] systems of Auger electron spectroscopy clearly demonstrate the segregation of one of the alloy constituents, gold and aluminum, respectively, in the topmost surface layer. These systems obey the regular solution model of surface composition. There are several contradictory reports on the surface composition in the Cu-Ni system. According to the regular solution models, enrichment of the surface in copper is expected. Copper enrichment was indeed reported by Sachtler et al[14,15,16] Helms, Yee and Spicer[17] and Burton et al.[18] Takasu and Shimizu[19] found copper enrichment at the surface of nickel-rich alloys while copper-rich alloys had excess nickel at the surface. Ertl and Kuppers[20] and Quinto et al[21] found the surface composition the same as the bulk. It appears that sample preparation must have had a controlling influence on the equilibration of the two components, copper and nickel, in this system. It is possible that the contradictory results are due to the phase segregation reported by Sachtler,[14] that would not permit the application of the regular solution model to this binary alloy.

There are many experimental parameters that may make studies of surface phase diagrams of alloys difficult. Adsorption of gases from the ambient or segregation of impurities by diffusion from the bulk to the surface can markedly change the surface composition. If any of the impurities form stronger bonds with one component as compared to the other, the strongly bound component will be pulled to the surface by the impurity segregated there. On removal of the impurity, the surface composition may change again indicating the re-equilibration of the pure surface phase with that of the bulk. For the small crystallites present in the alloy thin-films the surface composition can be influenced by the particle size. In the limit of small particle size the surface composition must approach the bulk composition since most of the atoms must then reside on the surface. As we have pointed out above, a large exothermic heat of mixing would indicate the tendency for layering or ordering near the surface that would disallow the use of the regular solution model.

It would, of course, be of great importance to study the surface composition of alloy systems with complex phase diagrams where ordering and compound formation occurs. Although there have been attempts to describe the surface composition of these complex alloy systems,[14,22] experimental data have been scarce. The surface composition of a wide variety of complex alloy systems must be studied before realistic thermodynamic models of their behavior can be developed.

It appears that for homogeneous binary systems with relatively small regular solution parameters, the surface phase diagram can be described adequately with a regular solution model of the monolayer type. Thus, one may use the monolayer regular solution model to predict the surface composition of homogeneous binary alloys.

5) ACKNOWLEDGMENT

This work was supported by the U.S. Energy Research and Development Administration.

REFERENCES

1. G. A. Somorjai, Principles of Surface Chemistry (Prentice-Hall, Englewood Cliffs, 1972).
2. R. Defay et al, Surface Tension and Adsorption (John Wiley & Sons, New York, 1966).
3. F. J. Szalkowski and G. A. Somorjai, Adv. High Temp. Chem., 1971, 4, 137.
4. F. Meyer and J. J. Vrakking, Surface Sci., 1972, 33, 271.
5. R. A. Swalin, Thermodynamics of Solids (John Wiley & Sons, New York, 2nd ed., 1972).
6. F. L. Williams, Surface Sci., 1974, 45, 377.
7. R. Hultgren et al, Selected Values of Thermodynamic Properties of Metals and Alloys (John Wiley & Sons, New York, 1963).
8. S. H. Overbury and G. A. Somorjai, J. of Chem. Rev., 1975, to be published.
9. C. J. Powell, Surface Sci., 1974, 44, 29.
10. S. Berglund and G. A. Somorjai, J. of Chem. Phys., 1973, 59, 5537.
11. S. H. Overbury and G. A. Somorjai, to be published.
12. F. L. Williams and M. Boudart, J. Catalysis, 1973, 30, 438.
13. J. Ferrante, Acta Metallurgica, 1971, 19, 743.
14. W. M. H. Sachtler and R. Jongepier, J. Catalysis, 1965, 4, 665.
15. W. M. H. Sachtler and G. J. H. Dorgelo, J. Catalysis, 1965, 4, 654.
16. W. M. H. Sachtler, J. Vac. Sci. and Tech., 1971, 9, 828.
17. C. R. Helms, K. Y. Yu and W. E. Spicer, 1975, to be published.
18. J. J. Burton and E. Hyman, J. Catalysis, 1975, in press.
19. Y. Takasu and H. Shimizu, J. Catalysis, 1973, 29, 479.
20. G. Ertl and J. Kuppers, J. Vac. Sci, and Tech., 1971, 9, 829.
21. D. T. Quinto, V. S. Sundaram and W. D. Robertson, Surface Sci., 1971, 28, 504.
22. R. A. Van Santen and W. M. H. Sachtler, J. Catalysis, 1974, 33, 202.

Figure 1. Surface enrichment for a (111) face in the Au-Ag system at 300°K as predicted by the monolayer regular and by the 4-layer regular solution models. The enrichment is plotted as a function of the bulk composition. In the 4-layer model, the enrichment in each layer is shown.

Figure 2. Same as Figure 1 except at 900°K.

Figure 3. The surface enrichment for a (111) face in the Pb-In system at 600°K as predicted by the monolayer regular and the 4-layer regular solution models. The enrichment is plotted against the alloy bulk composition. In the 4-layer model, the enrichment in each layer is shown. The surface composition predicted by the monolayer model is very similar to that predicted for the first layer of the 4-layer model.

Figure 4. Ratios of the In(403eV) to the Pb(92eV) intensities. The ratios are all divided by this ratio obtained from pure Pb and In. The multiple points for one alloy demonstrate the temperature dependence of this ratio. The dotted line gives the values expected for a surface with the same composition as that in the bulk.

Figure 5. Intensity ratio of the Au(72eV) to the Ag(356eV) peak. The ratios are all divided by the same ratio for pure Ag and Au and plotted as a function of the bulk composition ratios. The solid lines are predicted for a 4-layer regular solution model. The monolayer regular solution model gives essentially identical values. The dotted lines gives the values expected for a surface with the same composition as that in the bulk.

Figure 6. Same as Figure 5 except using the Au(241eV) peak and the Ag(356eV) peak.

Figure 7. The ratio of the Au(72eV) as predicted by the monolayer and the 4-layer regular solution models. The ratios are divided by the ratio obtained from pure Au. The dotted line is the value expected when the surface composition is identical to that in the bulk.

Figure 8. The sum of the normalized intensity ratios as predicted from the monolayer and the 4-layer regular solution models for the Ag-Au system. At 900°K the monolayer and 4-layer models give essentially identical results. The dotted line gives the value expected and the surface composition is the same as that in the bulk.

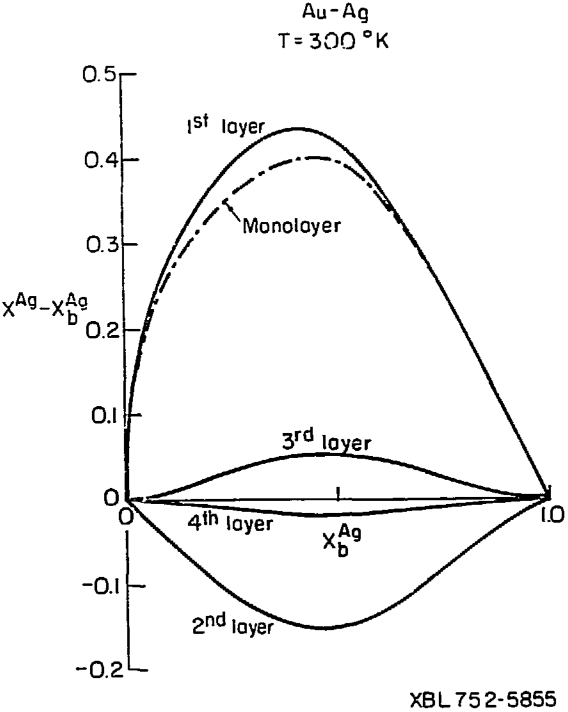
Au-Ag
T = 300 °K
0.5
0.4
0.3
0.2
0.1
0
-0.1
-0.2
$X^{Ag}-X_b^{Ag}$
1st layer
Monolayer
3rd layer
4th layer
2nd layer
0
1.0
X_b^{Ag}
XBL 752-5855

Fig. 1

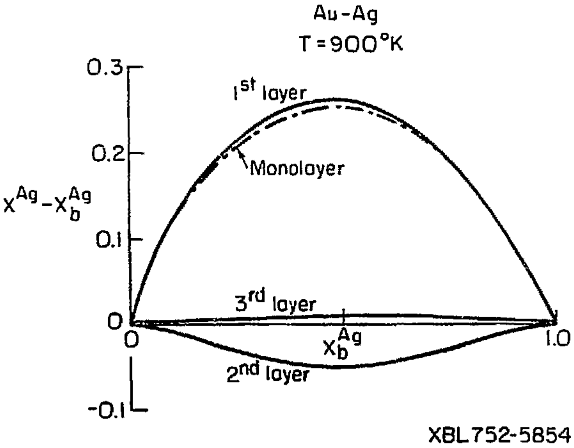
Au-Ag
T = 900°K
0.3
0.2
0.1
0
-0.1
$X^{Ag} - X_b^{Ag}$
1st layer
Monolayer
3rd layer
2nd layer
0
X_b^{Ag}
1.0
XBL 752-5854

Fig. 2

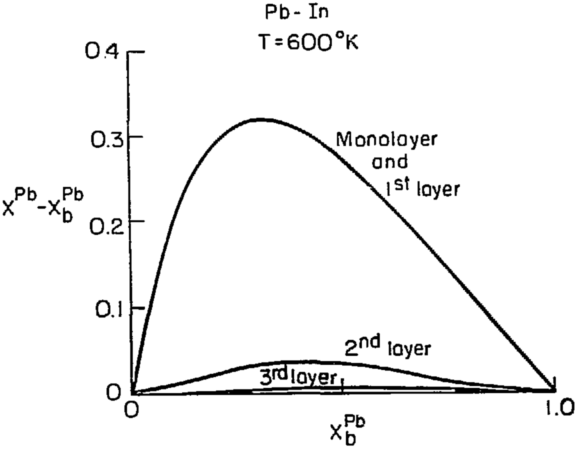

XBL752-5853

Fig. 3

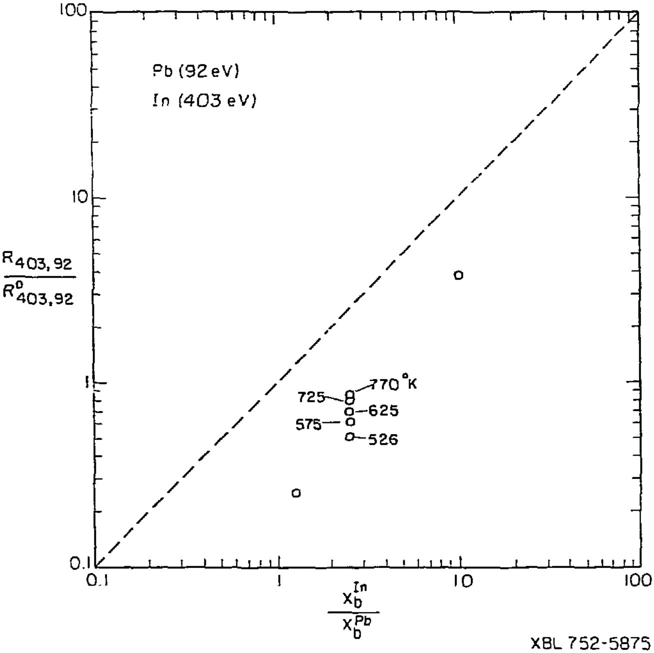
Pb (92 eV)
In (403 eV)
$\frac{R_{403,92}}{R^0_{403,92}}$
$\frac{X_b^{In}}{X_b^{Pb}}$
100
10
1
0.1
0.1
1
10
100
770 °K
725
625
575
526
XBL 752-5875

Fig. 4

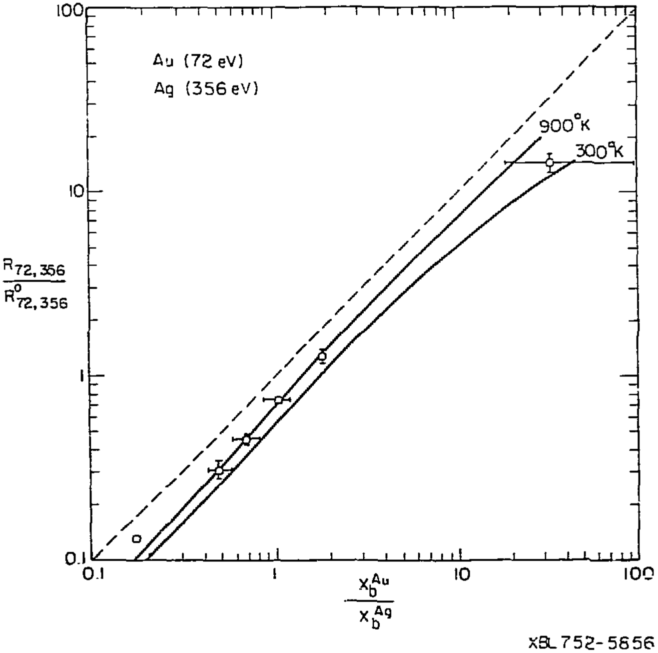
100
10
1
0.1
0.1
1
10
100
Au (72 eV)
Ag (356 eV)
900°K
300°K
$\frac{R_{72,356}}{R^{o}_{72,356}}$
$\frac{X_b^{Au}}{X_b^{Ag}}$
XBL 752-5856

Fig. 5

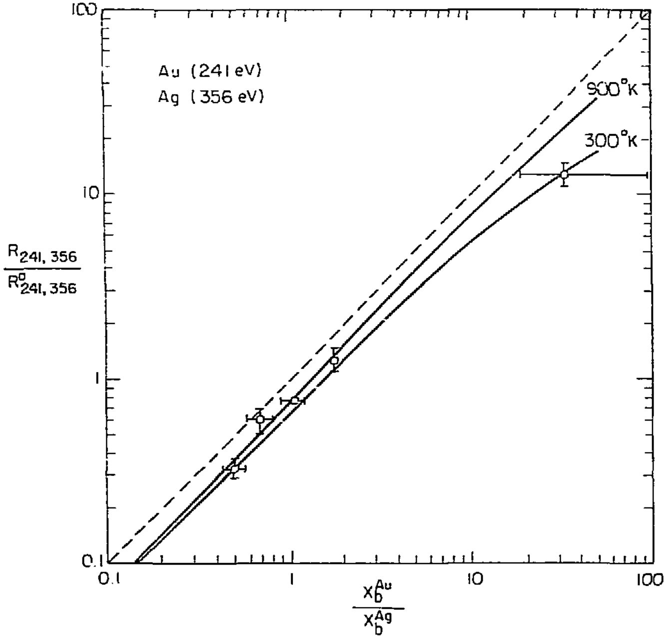

XBL 752-5857

Fig. 6

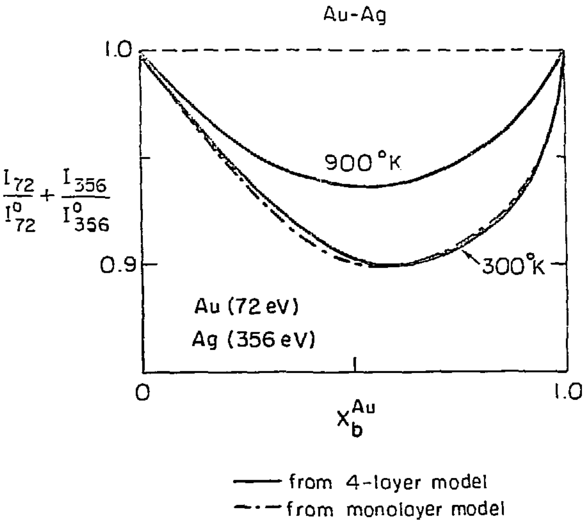

XBL 752-5851

Fig. 7

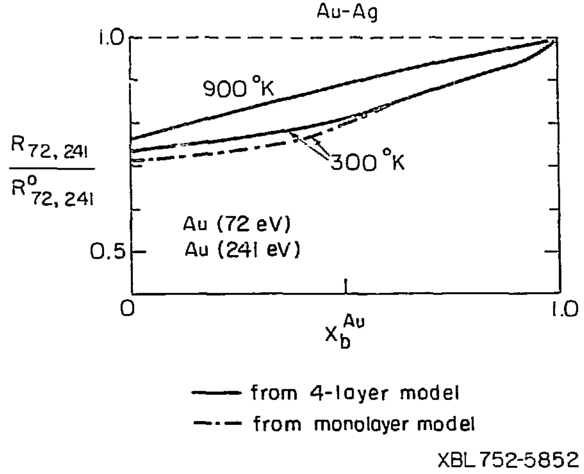
Au-Ag
1.0
0.5
0
1.0
$\frac{R_{72,241}}{R^{o}_{72,241}}$
X_b^{Au}
900 °K
300 °K
Au (72 eV)
Au (241 eV)
from 4-layer model
from monolayer model
XBL 752-5852

Fig. 8